32nd URSI GASS, Montreal, 19–26 August 2017

METHOD FOR DIRECT DETECTION OF PITCH ANGLE SCATTERING CAUSED BY PLASMA WAVES

Masahiro Kitahara*(1) and Yuto Katoh(1)
(1) Department of Geophysics, Graduate School of Science, Tohoku University

Abstract

We propose a new method to directly detect pitch angle scattering of energetic particles caused by plasma waves in space plasma. The Wave-Particle Interaction Analyzer (WPIA), a new instrument proposed by [1], measures the energy exchange from waves to particles. In this study, we expand its applicability to detect pitch angle scattering of resonant particles by plasma waves by calculating g values. g value is defined as the accumulation value of the Lorentz force acting on each particle and indicates the lost momentum of waves. We apply the proposed method to the results of a one-dimensional electron hybrid simulation reproducing the generation of whistler-mode chorus emissions around the magnetic equator [2, 3]. Using the wave and particle data obtained at fixed observation points assumed in the simulation system, we conduct a pseudo-observation of the simulation result using the WPIA and analyze the g values. Our analysis yielded significant values indicating the strong pitch angle scattering for electrons in the kinetic energy and pitch angle ranges satisfying the cyclotron resonance condition with the reproduced chorus emissions. The results of this study demonstrate that the proposed method enables us to directly and quantitatively identify the location at which pitch angle scattering occurs in the simulation system and that the method can be applied to the results of space-based observations by the Exploration of energization and Radiation in Geospace (ERG) satellite.

1 Introduction

Whistler-mode chorus emissions are often observed in the Earth's magnetosphere [4, 5]. Whistler-mode chorus emissions are generally characterized by a sequence of intense and coherent emissions with a frequency shift. Emissions with a positive or negative frequency sweep rate are called rising or falling tones, respectively, and rising tones are observed more frequently than falling tones. Pitch angle scattering of energetic electrons caused by whistler-mode chorus emissions is a significant wave-particle interaction in the Earth's magnetosphere. Previous studies suggested that whistler-mode chorus emissions play a dominant role in pitch angle scattering of energetic electrons in the kinetic energy range from a few to tens of keV, which is closely related to precipitation contributing to pulsating aurora [6].

On the JAXA satellite mission Exploration of energization and Radiation in Geospace (ERG), a software-type Wave-Particle Interaction Analyzer (WPIA) is installed to directly and quantitatively detect wave-particle interactions between whistler-mode chorus emissions and energetic electrons [7]. The WPIA is a new instrument proposed by [1] and measures the relative phase angle between the wave magnetic field vector and the velocity vector of each particle so as to calculate the energy exchange between waves and particles. $I = q\sum_i \boldsymbol{E}_w(t_i)\cdot\boldsymbol{v}_i$ is introduced as a measurable value obtained by the WPIA [1], where q, v_i, t_i, and $\boldsymbol{E}_w$ are the charge, velocity, and timing of the detection of the $i-$th particle, and the wave electric field vector as a function of time, respectively. The I value expresses the accumulated value of the time variation of the kinetic energy of particles corresponding to the Joule heat of resonance particles gained from plasma waves [8].

For direct measurement of pitch angle scattering, we should consider another physical value to measure using the WPIA. We reported a new method of directly and quantitatively detecting pitch angle scattering of energetic particles caused by plasma waves using the WPIA and its feasibility in [9], and this paper describes the brief summary of our previous studies.

2 Measurable Values of the WPIA

The pitch angle α is defined as

$$\alpha = \tan^{-1}\left(\frac{v_\perp}{v_\parallel}\right) = \tan^{-1}\left(\frac{p_\perp}{p_\parallel}\right), \tag{1}$$

where $v_\perp$ and $v_\parallel$ are the perpendicular and parallel components of the velocity vector $\boldsymbol{v}$ of a particle, respectively, and $p_\perp$ and $p_\parallel$ are the perpendicular and parallel components of the momentum vector $\boldsymbol{p}$, given by $\boldsymbol{p} = m\gamma\boldsymbol{v}$, respectively. m and γ are the rest mass of the particle and the Lorentz factor, respectively. Differentiating both sides of equation (1), we obtain the following equations:

$$\frac{\mathrm{d}\alpha}{\mathrm{d}t} = \frac{1}{p}\left(\frac{\mathrm{d}p_\perp}{\mathrm{d}t}\cos\alpha - \frac{\mathrm{d}p_\parallel}{\mathrm{d}t}\sin\alpha\right) = \frac{1}{p}\frac{\mathrm{d}\boldsymbol{p}}{\mathrm{d}t}\cdot\boldsymbol{e}_\alpha, \tag{2}$$

where $p = |\boldsymbol{p}|$, and $\boldsymbol{e}_\alpha$ is a unit vector defined as $\boldsymbol{e}_\alpha = \boldsymbol{e}_\perp\cos\alpha - \boldsymbol{e}_\parallel\sin\alpha$ (see Fig. 1).

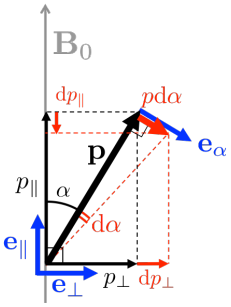

Figure 1. Geometric relationships among $\mathbf{p}$, $\mathbf{e}_{\parallel}$, $\mathbf{e}_{\perp}$, and $\mathbf{e}_{\alpha}$. Note that all vectors in this figure are defined in the $p_{\parallel}$–$p_{\perp}$ plain.

Equation (2) shows that the variation of the pitch angle with time is equal to the component of the time differentiation of the momentum along $\boldsymbol{e}_{\alpha}$. Because the time variation of the momentum is equal to the force acting on a particle, the pitch angle variation caused by wave-particle interaction is expressed by the Lorentz force due to wave electromagnetic fields. Equation (2) is rewritten as

$$F_{\alpha} = q\left(\boldsymbol{E}_w + \boldsymbol{v}\times\boldsymbol{B}_w\right)\cdot\boldsymbol{e}_{\alpha} = p\frac{\mathrm{d}\alpha}{\mathrm{d}t}. \tag{3}$$

To discriminate scattered particles from other particles, we define g as a function of $\boldsymbol{v}$ and time:

$$g(\boldsymbol{v},t) = q\left(\boldsymbol{E}_w + \boldsymbol{v}\times\boldsymbol{B}_w\right)\cdot\boldsymbol{e}_{\alpha} f(\boldsymbol{v},t). \tag{4}$$

Because g is the distribution of the amount of momentum exchange in the direction of varying pitch angle, $g(\boldsymbol{v},t)$ shows the time and the location in velocity space at which momentum is effectively exchanged between waves and particles. Because we define the pitch angle in a range from 0 to 180°, positive g in the range from 0 to 90° and negative g in the range from 90 to 180° show that particles are moving away from the loss cone, and negative g in the range from 0 to 90° and positive g in the range from 90 to 180° show that particles are moving toward the loss cone.

Practically, we calculate the g values from data for a finite number of particles. Let N be the number of particles in a finite energy range, in a finite solid angle range, and in a finite time interval in a unit area. Then the g value calculated from discrete data in energy-pitch angle space is expressed as

$$g(K,\alpha,t) = \frac{1}{2\pi\sin\alpha\Delta K\Delta\alpha\Delta t}\frac{m^2}{K}\frac{\gamma^5}{\gamma+1}\frac{1}{\boldsymbol{n}\cdot\hat{\boldsymbol{v}}}\sum_{\substack{K\le K_i\le K+\Delta K\\ \alpha\le\alpha_i\le\alpha+\Delta\alpha\\ t\le t_i\le t+\Delta t}}^{N}(F_{\alpha})_i, \tag{5}$$

where m, $\boldsymbol{n}$, and $\hat{\boldsymbol{v}}$ are the rest mass of the particles, the normal vector to the detection plane, and a unit vector in the direction of $\boldsymbol{v}$, respectively, and $(F_{\alpha})_i = q\left(\boldsymbol{E}_w(t_i) + \boldsymbol{v}_i\times\boldsymbol{B}_w(t_i)\right)\cdot(\boldsymbol{e}_{\alpha})_i$, where i is the particle index, and t_i is the time at which the i-th particle is detected. For the details of the derivation of equation (5), see Appendix of [9]. If the waves scatter the pitch angle of electrons and then the distribution function f in the ϕ direction is modulated on a time scale corresponding to the wave frequency, g integrated over ϕ is expected to show a significant value. In contrast, if there are no wave-particle interactions, g is negligible small.

The g value contains statistical fluctuations because it is calculated by accumulating a finite number of particles. According to the central limit theorem, because we can assume that the accumulated g follows a normal distribution function, we can estimate the fluctuation of the g value by evaluating the standard deviation of the distribution, which is given by

$$\sigma_g(K,\alpha,t) = \Lambda\sqrt{\sum_{\substack{K\le K_i\le K+\Delta K\\ \alpha\le\alpha_i\le\alpha+\Delta\alpha\\ t\le t_i\le t+\Delta t}}^{N}\left((F_{\alpha})_i\right)^2 - \frac{1}{N}\left(\sum_{\substack{K\le K_i\le K+\Delta K\\ \alpha\le\alpha_i\le\alpha+\Delta\alpha\\ t\le t_i\le t+\Delta t}}^{N}(F_{\alpha})_i\right)^2}, \tag{6}$$

where $\Lambda = m^2\gamma^5/[2\pi\sin\alpha\Delta K\Delta\alpha\Delta t K(\gamma+1)\boldsymbol{n}\cdot\hat{\boldsymbol{v}}]$.

In this study, using equations (5) and (6), we apply the method to simulation results of purely parallel propagating whistler-mode waves generated by energetic electrons. The details of the data set are described in the next section.

3 Simulation

We analyzed the simulation results in order to evaluate the feasibility of the method proposed in the previous section. By a spatially one-dimensional electron hybrid simulation in an inhomogeneous ambient magnetic field, [2, 3] reproduced the generation process of whistler-mode chorus emissions in the region close to the magnetic equator. Chorus emissions emerge from a band of whistler-mode waves excited by an instability driven by a temperature anisotropy of energetic electrons and are generated by nonlinear wave-particle interactions [10, 11]. The initial distribution function of anisotropic energetic electrons is given by the loss cone distribution constructed by summing the bi-Maxwellian distributions. For the details of the numerical scheme and initial conditions used in the simulation, see [2, 3].

We analyzed the result of a simulation conducted using the same parameters as in [2, 3]. Two pseudo-observation points were fixed in the simulation box at $h = \pm 200\ c\Omega_e^{-1}$, corresponding to the locations at which the magnetic latitude is about ±8° at $L = 4$, where c and Ω_e are the speed of light and gyro-frequency of electrons, respectively. We analyzed the wave electromagnetic fields at these points and the velocity of particles that passed through them at each time step. Because the simulation system is spatially one-dimensional, waves generated in the simulation are in the field-aligned propagation mode and are purely electromagnetic. Therefore, we used four components of the wave

electromagnetic fields (E_x, E_y, B_x, and B_y), which are perpendicular to the ambient magnetic field $\boldsymbol{B}_0$, in the analysis. The velocity of the particles is computed in three dimensions; therefore, we used three velocity components (v_x, v_y, and v_z) detected at each time step. Henceforth, the points at $h = +200\ c\Omega_e^{-1}$ and $h = -200\ c\Omega_e^{-1}$ are called points A and B, respectively.

4 Results and Discussion

Figs. 2 (a) and (b) show wave magnetic field spectra at the fixed points A and B, respectively. Rising tone chorus emissions are reproduced in the simulation system. In this simulation, chorus emissions are generated from the initial thermal noise of energetic electrons near $h = \pm 0\ c\Omega_e^{-1}$, corresponding to the magnetic equator, and propagate away from the equator as their amplitude increases nonlinearly [2].

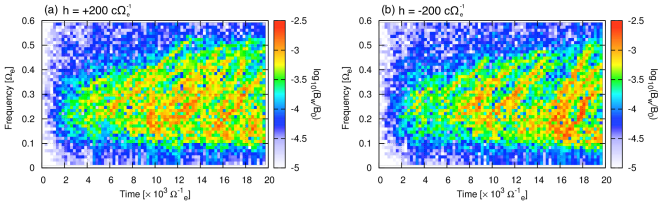

Figure 2. Wave magnetic field spectra measured at fixed points A and B in the simulation system.

Figs. 3 (a) and (b) show the evolution of the pitch angle distribution of electrons in the kinetic energy range of 180–220 keV at points A and B, respectively. We find streaky oblique lines in the temporal variation of the pitch angle distribution. The time step at which the lines appeared and the duration of each line correspond closely to those of rising tones appearing in the wave spectra. These results suggest that the variations in the pitch angle distribution are caused by chorus emissions generated in the simulation result. However, the amount of variation in the pitch angle distribution is almost always less than several percent of the total pitch angle distribution.

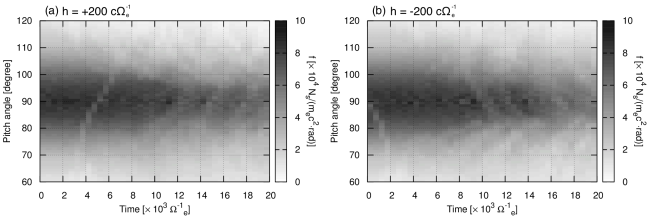

Figure 3. Temporal variation of the pitch angle distribution $f(t,\alpha)$ measured at points A and B.

Figs. 4 (a) and (b) show the g values obtained at each time interval in the corresponding pitch angle range. We use energetic electrons in the same energy range as in Fig. 3, and we plot only the g values satisfying the condition $g > 2\sigma_g$ in order to show the statistically significant results. Warm and cool colors indicate pitch angle increases and decreases, respectively. At point A in the northern hemisphere, we obtained positive g values at pitch angles greater than 90°. On the other hand, we obtained negative g values at pitch angles less than 90° at point B in the southern hemisphere. Although we found similar variations in the pitch angle distribution at points A and B (see Fig. 3), Figs. 4 (a) and (b) clearly differentiate the pitch angle range in which significant pitch angle scattering occurred at points A and B. These results reveal that the g values successfully clarified the location at which pitch angle scattering occurred and the pitch angle range in which energetic electrons are effectively scattered by the waves.

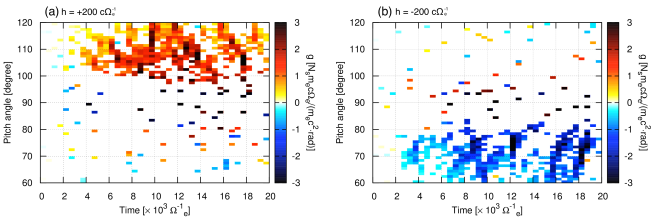

Figure 4. Temporal variation of g as a function of pitch angle at $K = 200 \pm 20$ keV. To show the statistically significant values, we plot only the g values satisfying the condition $g > 2\sigma_g$.

Figs. 5 (a) and (b) show the g values in K–α space calculated at points A and B, respectively. In the result shown in Fig. 5, we used particles detected in the entire simulation time, which corresponds to the time interval from 0 to 20,000 Ω_e^{-1}. The color bar in Fig. 5 is the same as that in Fig. 4. Black solid lines in Fig. 5 are the resonance curves corresponding to each frequency, which are expressed as

$$\omega - kv\cos\alpha = \frac{\Omega_e}{\gamma}, \tag{7}$$

where ω and k are the wave angular frequency and wave number, respectively. According to [2], electrons at energies from 100 keV to several hundreds of keV generate whistler-mode chorus emissions, and MeV electrons are accelerated by chorus emissions. Figs. 5 (a) and (b) indicate that electrons at kinetic energies from 100 keV to a few MeV are strongly scattered, and their pitch angle shifts away from 90°.

We examine the resonance condition using the parameters in the simulation. For $k > 0$ (northward propagation), waves in the frequency range $0.1 < \omega/\Omega_e < 0.5$ can resonate with electrons having a kinetic energy of 200 keV and pitch angle range of $93° < \alpha < 118°$. For $k < 0$ (southward propagation), waves in the frequency range of $0.1 < \omega/\Omega_e < 0.5$ can resonate with 200 keV electrons in the pitch angle range of $62° < \alpha < 87°$. The pitch angle ranges in which statistically significant g values are obtained in Fig. 4 are con-

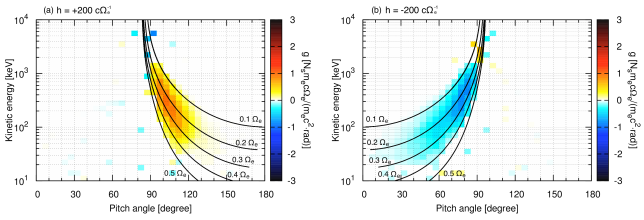

Figure 5. The g values in the K–α space calculated at fixed points over the time interval from 0 to 20,000 Ω_e^{-1}.

sistent with these estimations of the resonance condition, and the statistically significant g values in Fig. 5 are also consistent with the resonance conditions for each frequency (black lines in Fig. 5). Namely, we can discriminate scattered particles and other particles by measuring the g values at the observation point at the observation time.

5 Summary

We proposed a new method of detecting pitch angle scattering using the WPIA by [9]. The time variation of the pitch angle is formulated as the time variation of the momentum, which is the Lorentz force in the direction of increasing pitch angle, and the measurable value g is defined as the direction of varying pitch angle component of the lost momentum of the wave electromagnetic fields. We applied the proposed method to simulation results reproducing the generation of whistler-mode chorus emissions and evaluated the feasibility of the proposed method. Pseudo-observations at fixed points in the simulation system indicate that the time variation of the pitch angle distribution of electrons is very small, but the g values clearly show the statistically significant results of pitch angle scattering. The simulation results clarified that the proposed method enables us to identify the location at which pitch angle scattering occurs and the energy and pitch angle ranges in which energetic electrons are effectively scattered. A significant future work is the application of the proposed method to observation data obtained the ERG satellite. Direct measurements in space plasma will provide important clues to the study of processes governing pitch angle scattering of energetic particles in the magnetosphere.

6 Acknowledgements

The computer simulation was performed on the KDK computer system at the Research Institute for Sustainable Humanosphere, Kyoto University and the computational resources of the HPCI system provided by the Research Institute for Information Technology, Kyushu University, the Information Technology Center, Nagoya University, and the Cyberscience Center, Tohoku University through the HPCI System Research Project (Project ID: hp160131). This study is supported by Grants-in-Aid for Scientific Research (15H05815, 15H05747, 15H03730) of Japan Society for the Promotion of Science and a joint research program at the Institute for Space-Earth Environmental Research, Nagoya University.

References

[1] Fukuhara, H. et al. (2009), A new instrument for the study of wave–particle interactions in space: One-chip Wave–Particle Interaction Analyzer, *Earth Planets Space*, 61, 765.

[2] Katoh, Y., and Y. Omura (2007a), Computer simulation of chorus wave generation in the Earth's inner magnetosphere, *Geophys. Res. Lett.*, 34, L03102, doi:10.1029/2006GL028594.

[3] Katoh, Y., and Y. Omura (2007b), Relativistic particle acceleration in the process of whistler–mode chorus wave generation, *Geophys. Res. Lett.*, 34, L13102, doi:10.1029/2007GL029758.

[4] Tsurutani, B. T., and E. J. Smith (1974), Postmidnight chorus: A substorm phenomenon, *J. Geophys. Res.*, 79(1), 118, doi:10.1029/JA079i001p00118.

[5] Santolik, O. et al. (2003), Spatio-temporal structure of storm-time chorus, *J. Geophys. Res.*, 108(A7), 1278, doi:10.1029/2002JA009791.

[6] Nishimura, Y. et al. (2010), Identifying the driver of pulsating aurora, *Science (New York, N.Y.)*, 330(6000), 81, doi:10.1126/science.1193186.

[7] Miyoshi, Y. et al. (2012), The Energization and Radiation in Geospace (ERG) Project, in: Dynamics of the Earth's Radiation Belts and Inner Magnetosphere, Geophys. Monogr. Ser., 199, edited by: D. Summers, I. R. Mann, D. N. Baker, and M. Schulz, 103–116, AGU, Washington, D.C., doi:10.1029/2012GM001304.

[8] Katoh, Y. et al. (2013), Significance of Wave–Particle Interaction Analyzer for direct measurements of nonlinear wave–particle interactions, *Ann. Geophys.*, 31, doi:10.5194/angeo-31-503-2013.

[9] Kitahara, M., and Y. Katoh (2016), Method for direct detection of pitch angle scattering of energetic electrons caused by whistler mode chorus emissions, *J. Geophys. Res.*, 121, doi:10.1002/2015JA021902.

[10] Omura, Y. et al. (2008), Theory and simulation of the generation of whistler–mode chorus, *J. Geophys. Res.*, 113, doi:10.1029/2007JA012622.

[11] Omura, Y. et al. (2009), Nonlinear mechanisms of lower-band and upper-band VLF chorus emissions in the magnetosphere, *J. Geophys. Res.*, 114, doi:10.1029/2009JA014206.